

## FATIGUE CRACK INITIATION AND PROPAGATION FROM ANGLED WELD CRACKS

*By Takeshi MORI\* and Hideo TOKIDA\*\**

In order to examine the properties of fatigue crack initiation and propagation from weld cracks which were created at high temperature and also to make clear the influence of weld crack angle on the above mentioned properties, fatigue tests were performed on the specimens containing the weld cracks of various orientations. The material used was JIS SM50A steel. Weldings were done by submerged arc processes or metal-inert-gas arc processes. The specimens were bending-type which contained cracks on the edge, and tension-type which possessed cracks on the center. The angles between crack orientations and applied stress direction were 90, 60, 30 degrees in the bending-type specimens, and were 90, 60, 45 degrees in the tension-type specimens.

*Keywords: weld crack, fatigue crack, initiation, propagation, threshold condition*

### 1. INTRODUCTION

The determination of whether planar weld defects such as weld cracks and lack of penetration are allowable or are to be subjected to repairs, is often done by applying the techniques of fracture mechanics<sup>1)~3)</sup>. For example, in the British recommendation BSI PD 6493, the assessment is based on the fatigue crack propagation life which is calculated by using the relationship between crack propagation rate ( $da/dN$ ) and stress intensity factor range ( $\Delta K$ ) incorporated with the threshold stress intensity factor range for crack propagation ( $\Delta K_{th}$ ). In this calculation, the defects are regarded as real cracks. Hence, the threshold condition for crack initiation from these defects, which is related to the fatigue limit, is assumed to be the same as the condition for fatigue crack propagation. Furthermore, the relationship between  $da/dN$  and  $\Delta K$  is obtained by subjecting structural steel, weld metal and heat-affected zones to fatigue crack propagation tests.

Weld cracks often occur along the weak orientations in weld metals, which results in the probability that the  $da/dN$ - $\Delta K$  relationship and the threshold condition for crack initiating from weld crack differ from those in normal weldments. Therefore, in order to assess the permissible size of weld cracks rationally, it is necessary to make ascertain the threshold condition for crack initiation and the rate of crack propagation from weld cracks. It is especially important to compare the threshold conditions for crack initiation from the weld crack and crack propagation in normal weldments. Furthermore, weld cracks occur in various orientations to stress direction. In this case, the threshold condition for fatigue crack initiation and  $da/dN$ - $\Delta K$  relationship from angled crack should be verified.

\* Member of JSCE, Dr. Eng., Research Associate, Dept. of Civil Eng., Tokyo Institute of Technology (2-12-1 O-okayama, Meguro-ku, Tokyo 152)

\*\* Member of JSCE, M. Eng., Ishikawajima-Harima Heavy Industry (5-17 Hikari-cho Kure-shi Hiroshima 737)

In this study, the properties of fatigue crack initiation and propagation from weld cracks occurring in weld metals are examined. The influence of weld crack angles on these properties is also discussed.

## 2. EXPERIMENTAL PROCEDURE

The material used was JIS SM50A steel of 45 mm thick. Chemical compositions and mechanical properties of this material are shown in Table 1. Weld cracks were introduced by controlling the configuration of weld groove (see Fig. 1) and conditions of welding. Welding processes and conditions used are as shown in Table 2. The weld crack in this study was created at high temperature, and its tip was blunt (see Fig. 4 and 5). This crack is generally called as "hot cracking". The lengths of the weld cracks were from 1 to 4 mm, and radius of the crack tip ranged from 0.04 to 0.15 mm.

Specimens were composed of two types, one was the bending-type specimen containing a weld crack on the edge, and the other was the tension type specimen with a weld crack on the center. The angles between the weld crack orientation and the stress direction were 90, 60 and 30 degrees in the bending-type specimen, and were 90, 60 and 45 degrees in the tension-type specimen. Hereafter, these specimens will be respectively indicated by the terms : B 90, B 60, B 30 specimen and T 90, T 60, T 45 specimen. The configurations and dimensions of these specimens are shown in Fig. 2.

Fig. 3 shows the distribution of welding residual stresses in the B 90 and T 90 specimens. These values were obtained by dissection method whereby strain gauges were adhered onto the surface of predicted location of fatigue crack propagation. The gauge length was 1 mm and the gauges were pasted at 5 mm intervals apart. The site of the weld crack is also shown in Fig. 3. The residual stress near the tip of the weld crack is tensile in the bending-type specimen and is compressive in the tension-type specimen. In order to remove or lower these stresses, post weld heat treatment (PWHT) was carried out on some of the specimens. This treatment was performed as follows. First the specimen was heated to 580°C at the rate of 100°C/hr, after which the specimen was maintained this temperature for 2 hours, then cooled down to room temperature at the rate of 100°C/hr.

Electro-hydraulic servo-system fatigue testing machine with a dynamic capacity of 50 kN was used. Load waveform was sinusoidal and its cyclic rate ranged from 10 to 30 Hz. Three points bending tests with a span of 160 mm were performed on the bending-type specimens. Stress ratio was set at about 0.1 in both the bending and tension-type specimens. If the number of stress cycles reached either  $10^6$  or  $2 \times 10^6$  and fatigue crack was not observed, the stress ranges was increased by 5 to 10% and tests were continued. Measurements of fatigue crack length were performed by making a replica of the fatigue cracked surface and observing the replica under the magnifying projector at 50 magnifications. The replica was made of acetate cellulose. By using this method, it was possible to measure the crack length to the accuracy of about 0.01 mm.

Table 1 Chemical Composition and mechanical properties of steel.

C	Si	Mn	P	S
x 100 (wt%)				
0.15	0.41	1.33	0.024	0.003
yield stress (MPa)		tensile strength (MPa)	elongation (%)	
360		560	34	

Table 2 Welding process and conditions.

specimen	welding process	welding condition			
		current (A)	voltage (V)	speed (cm/min)	heat input (kJ/cm)
B90, T90	submerged-arc process wire : US-36(4.8 $\phi$ ) flux : G6A	750	28	48	26.3
B60, T60	MIG process wire : MG-50T(1.2 $\phi$ ) shield gas : Ar(80%)+CO <sub>2</sub> (20%)	360	34	35	21.0
B30, T30	MIG process wire : MG-50T(1.2 $\phi$ ) shield gas : Ar(80%)+CO <sub>2</sub> (20%)	360	32	53	13.0

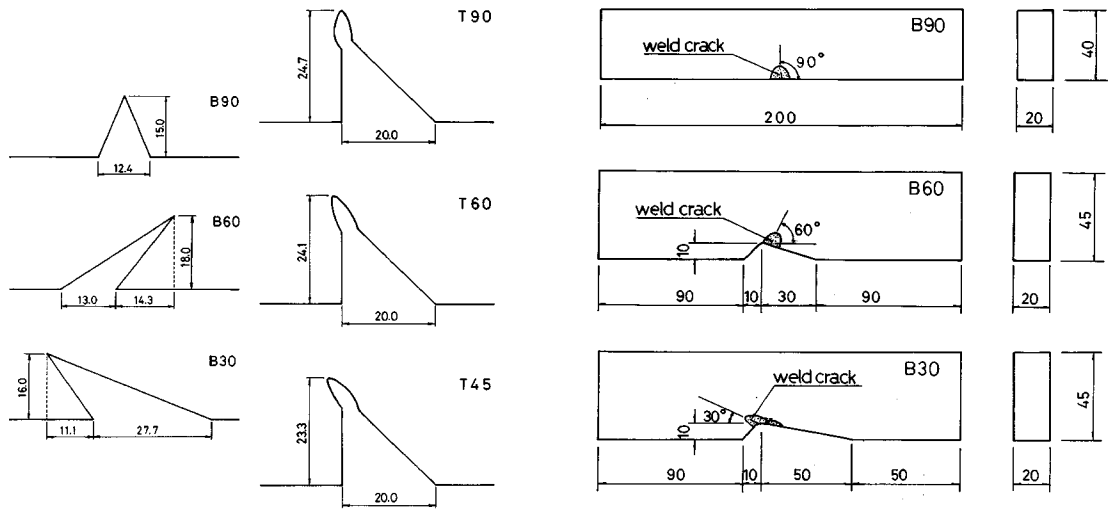


Fig. 1 Configuration of weld groove.

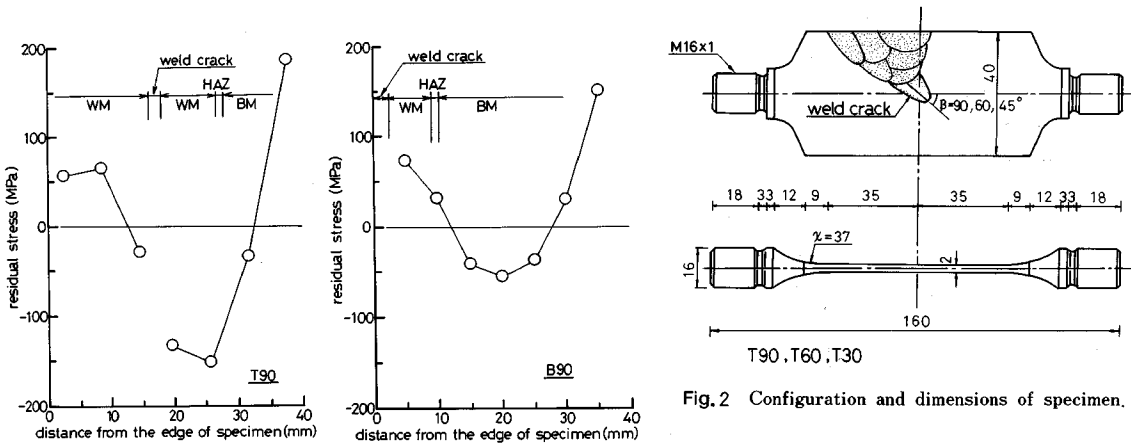


Fig. 3 Distribution of welding residual stress.

### 3. PROPERTIES OF FATIGUE CRACK INITIATION AND PROPAGATION

Photographs of B 90, B 60 and B 30 specimens with weld cracks and fatigue cracks are shown in Fig. 4. Fig. 5 shows the microscopic view of the weld crack tips and fatigue cracks (As the B 90 specimen indicated was subjected to post weld heat treatment, its fatigue crack width is narrower compared to those of B 60 and B 30 specimens). The fatigue crack in B 90 specimen initiated and propagated linearly along the interface of the columnar structures in the direction of the weld crack. In the case of B 60 and B 30 specimens, the fatigue crack propagated linearly across the columnar structures. However, a microscopic view of the area around the fatigue crack initiation point indicates that the fatigue crack initiated from the deepest point in the weld crack, and the crack orientation changed slightly when the crack length reached 0.2 to 0.4 mm. As shown above, the relationship between the directions of crack propagation and of the columnar structures varied according to the orientation of the weld crack, and in all cases, a macroscopic view indicated that the fatigue crack propagated perpendicularly to the stress direction.

The relationship between the weld crack angle  $\beta$  (the angle between the weld crack and stress direction, see Fig. 7) and crack initiation angle  $\theta_0$  (defined in Fig. 7), as obtained from these experiments, is shown in Fig. 6. As  $\beta$  gets larger,  $\theta_0$  becomes smaller. In addition,  $\theta_0$  in the tension-type specimen with a center

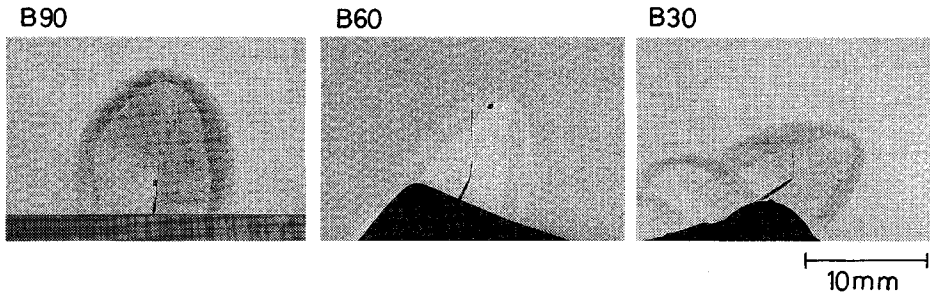


Fig. 4 Photographs of weld cracks and fatigue cracks.

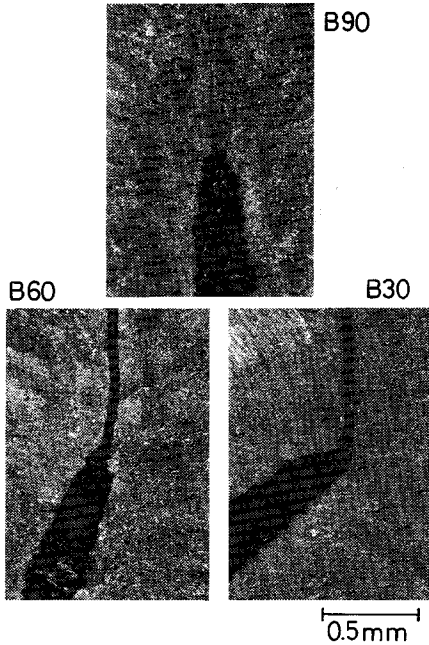


Fig. 5 Microscopic photographs of the region near fatigue crack initiation.

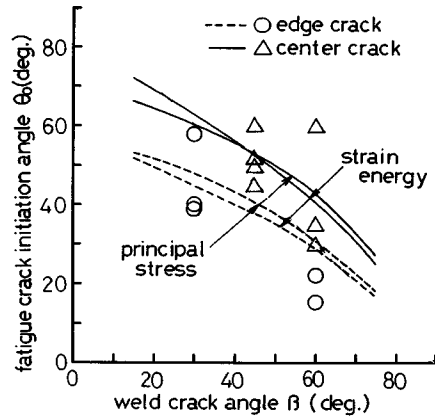


Fig. 6 Fatigue crack initiation angle from a weld crack.

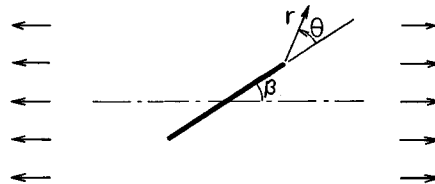


Fig. 7 Definition of co-ordinates.

weld crack is larger than  $\theta_0$  in the bending-type specimen with an edge weld crack.

The solid line in Fig. 6 indicates the crack initiation angle predicted by the maximum principal stress method and the minimum strain energy density criterion, using the stress intensity factors  $K_I$  and  $K_{II}$  of the angled crack in the infinite plate. The broken line was also similarly obtained, but here  $K_I$  and  $K_{II}$  were assumed to be the stress intensity factor of the angled edge crack in a semi-infinite plate. In which, following equations<sup>(4,5)</sup> were used to obtain the predicted relationships.

$$\left. \begin{aligned} \sigma_r &= 1/2 \sqrt{2\pi r} \times [K_I (3 - \cos \theta) \cos(\theta/2) + K_{II} (3 \sin \theta - 1) \sin(\theta/2)] + \dots \\ \sigma_\theta &= 1/2 \sqrt{2\pi r} \times \cos(\theta/2) [K_I (1 + \cos \theta) - 3 K_{II} \sin \theta] + \dots \\ \tau_{r\theta} &= 1/2 \sqrt{2\pi r} \times \cos(\theta/2) [K_I \sin \theta + K_{II} (3 \cos \theta - 1)] + \dots \end{aligned} \right\} \dots \dots \dots (1)$$

$$\partial (dW/dA) / \partial \theta = 1/r (a_{11} K_I^2 + a_{12} K_I K_{II} + a_{22} K_{II}^2) = 0 \dots \dots \dots (2)$$

$K_I, K_{II}$  : stress intensity factor for mode I, II

$dW/dA$  : strain energy density,  $a_{11}, a_{12}, a_{22}$  : material constant and function of  $\theta$

The predicted results express well the tendency of the experimental results. Therefore, it can be said that the direction of crack propagation is determined by the stress conditions near the crack tip, and is not influenced by the orientation of the columnar structures of the weld metal.

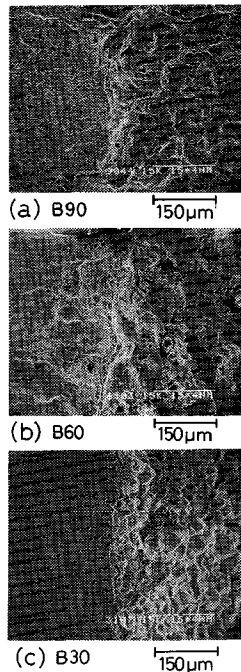


Fig. 8 Fatigue failure surface near the fatigue crack initiation point.

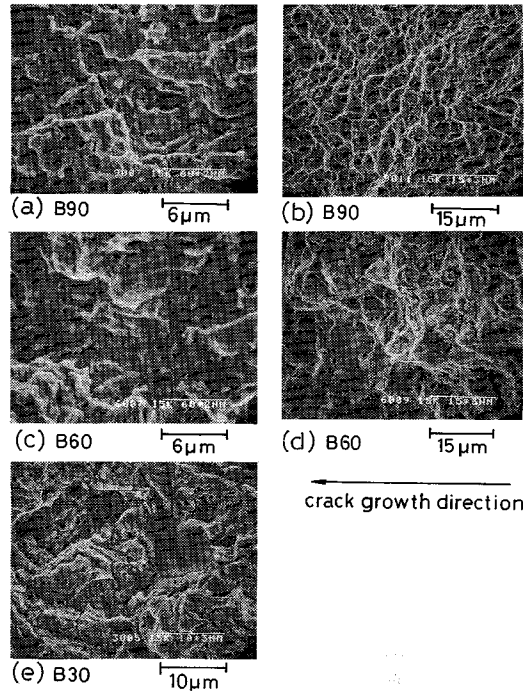


Fig. 9 Fatigue failure surface in weld metal.

The appearances of the region near the area of fatigue crack initiation in B 90, B 60 and B 30 specimens are shown in Fig. 8. In all the photographs, the right portion shows the weld crack and the left shows the fatigue-failed surface. Regardless of the type of specimen, the weld crack surface was strongly influenced by the columnar structures and intergranular surfaces are to be observed. However, the intergranular surfaces are not observed on the fatigue-failed surface. From this, it can therefore be said that the direction of fatigue crack initiation is not influenced by the orientation of the columnar structures of the weld metal.

The failure surfaces of the weld metals in B 90, B 60 and B 30 specimens are shown in Fig. 9. Macroscopically, the fatigue crack in B 90 specimen propagated along the interface of the columnar structures. However, as shown in Fig. 9 (a), transgranular failure surface was dominant, and intergranular failure surface was not observed so much. Furthermore, as shown in Fig. 9 (b), dimples was also observed in the B 90 specimen. As shown in Fig. 9 (c), in the B 60 and B 30 specimens, where the fatigue crack extended across the columnar structures, transgranular failure surface such as elastic striation was dominant. Also, as shown in Fig. 9 (d) and (e), in those two specimens, intergranular failure surface was partly observed. These observations indicate that the direction of fatigue crack growth is not dependent on the orientation of columnar structures.

#### 4. THE RATE OF FATIGUE CRACK PROPAGATION

Fig. 10 shows the relationship between fatigue crack propagation rate ( $da/dN$ ) and stress intensity factor range ( $\Delta K$ ) for fatigue crack propagation through weld metal. For B 60 and B 30 specimens,  $\Delta K$  was calculated as follows. The crack was projected in the direction of stress and then assumed to be a crack perpendicular to the stress direction. As shown in the previous section, in the case of angled weld crack, the fatigue crack also propagated perpendicularly to the stress direction. It has already been verified that the mode I stress intensity factor of this kinked crack is almost equal to that of the linear crack<sup>6</sup>. The

solid line in Fig. 10 shows the average relationship between  $da/dN$  and  $\Delta K^n$ . The results were obtained from a series of tests on SM 50 steel. As shown in Fig. 4, the fatigue crack in B 90 specimen propagated along the orientation of the columnar structure while those of B 60 and B 30 specimens grew across the structure. However, the  $da/dN$ - $\Delta K$  relationships of these specimens are almost identical. It can therefore be said that differences in the relationship between fatigue crack orientation and columnar structure orientation do not affect the  $da/dN$ - $\Delta K$  relationship. Furthermore, these  $da/dN$ - $\Delta K$  relationships are almost identical to that for SM 50 steel.

Fig. 11 shows the  $da/dN$ - $\Delta K$  relationship of a B 90 specimen for the cases when the fatigue crack pass through the weld metal (WM), the heat affected zone (HAZ) and the base metal (BM). The  $da/dN$  in

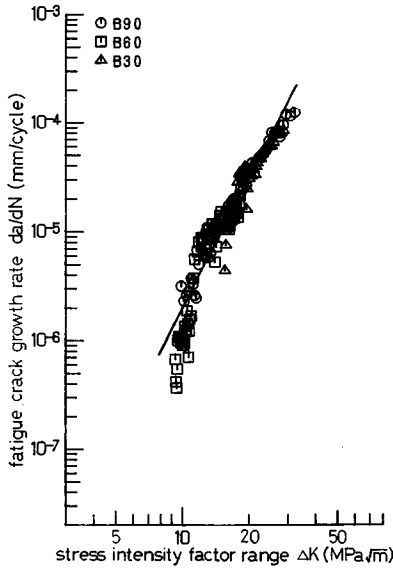


Fig. 10 Influence of weld crack angle on fatigue crack propagation rate in weld metal.

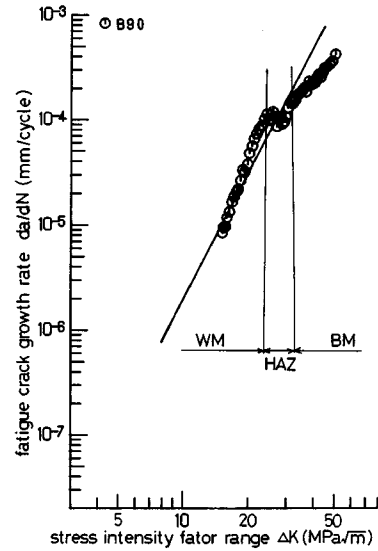


Fig. 11 Fatigue crack propagation rate in weld metal, heat affected zone and base metal.

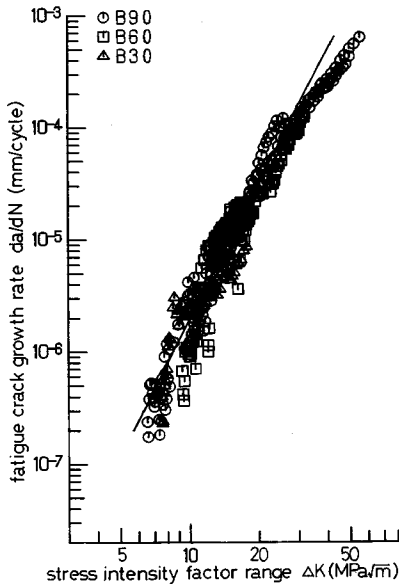


Fig. 12  $da/dN$ - $\Delta K$  relationship of bending-type specimens.

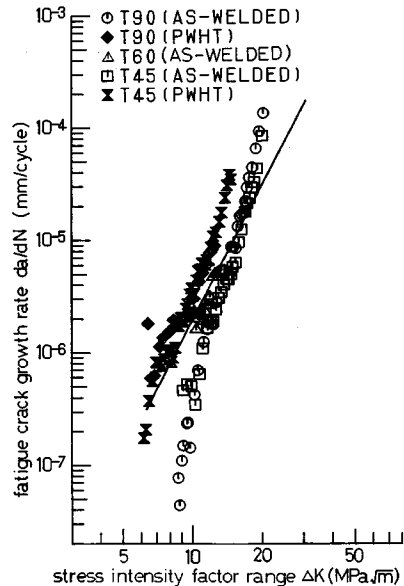


Fig. 13  $da/dN$ - $\Delta K$  relationship of tension-type specimens.

HAZ is low compared with those in WM and BM, but this difference is very slight. This fact suggests that the rates of fatigue crack growth are nearly equal in WM, HAZ and BM. The same phenomenon was also observed in B 60 and B 30 specimens. The data of the  $da/dN-\Delta K$  relationship obtained from the all of bending-type specimens, which include the data for crack propagation through WM, HAZ and BM, are shown in Fig. 12.

The  $da/dN-\Delta K$  relationships obtained from tension-type specimens are shown in Fig. 13. In the calculation of  $\Delta K$  for T 60 and T 45 specimens, the kinked crack was regarded as a linear crack. The solid markings in the figure show the  $da/dN-\Delta K$  relationships for post weld heat treated specimens. The  $da/dN-\Delta K$  relationships for these specimens are not influenced by the angle of weld crack and are expressed in the linear relationship. This linear relationship is almost identical to the average relationship for SM 50 steel. On the other hand, specimens not subjected to post weld heat treatment have very low  $da/dN$  value in the region of a short crack and a low  $\Delta K$ -value. This phenomenon can be considered to be caused by the compressive welding residual stress near the weld crack tip.

### 5. THRESHOLD CONDITION FOR FATIGUE CRACK INITIATION

The relationship between stress intensity factor range ( $\Delta K$ ) for weld crack and fatigue crack initiation life ( $N_i$ ) for both bending and tension-type specimens are shown in Fig. 14. In the case of angled cracks,  $\Delta K$  value is calculated by regarding the angled crack as a linear crack perpendicular to the stress direction.  $N_i$  is defined as the stress cycles required for the fatigue crack length to reach 0.5 mm. The marks with arrows in this figure indicate stress cycles at which fatigue crack was not observed. If the fatigue crack length reaches 0.05 mm, the existence of the crack will definitely be observed. The marks with arrows therefore indicate that, at the corresponding  $\Delta K$  value, the rate of fatigue crack propagation is less than  $5 \times 10^{-8}$  mm/cycle.

According to Fig. 14, for the initiation of fatigue crack from weld crack, the threshold value of stress intensity factor ranges from 5 to 8  $\text{MPa}\sqrt{\text{m}}$ . In the case of as-welded tension-type specimens, where there is a compressive residual stress field near the crack tip, the threshold value is slightly higher than those of bending-type specimens. However, the difference of threshold value is not influenced by the difference in angle of weld crack. In this experiment, the stress ratio ( $R$ ) was set at almost 0.1. The threshold value for crack propagation ( $\Delta K_{th}$ ) is about  $6\text{MPa}\sqrt{\text{m}}$  in the case of plain steel at  $R=0.1$  and is  $2\sim 3\text{MPa}\sqrt{\text{m}}$  in the case of welded joints with high tensile residual stress field<sup>8)</sup>. The threshold value obtained in this experiment is almost equal to the  $\Delta K_{th}$ -value for plain steel and is higher than the  $\Delta K_{th}$ -value for welded joint. It is therefore safe to predict the threshold value for fatigue crack initiation from the weld crack by

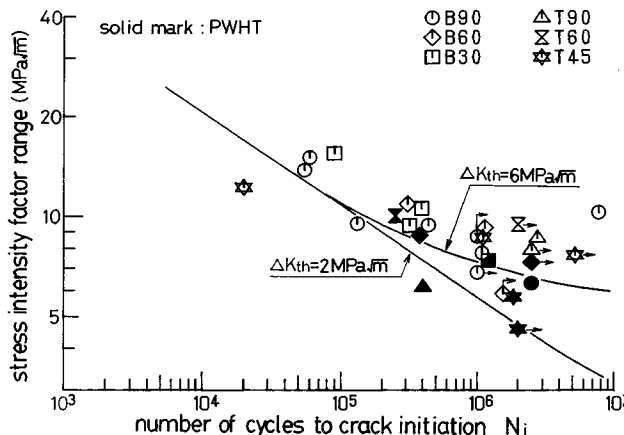


Fig. 14 Fatigue crack initiation life.

using  $\Delta K_{th}$ -value.

The solid line in Fig. 14 shows the calculated value of fatigue crack initiation life (see definition above). In this calculation, the following  $da/dN-\Delta K$  relationship<sup>7)</sup> was used.

$$da/dN = 1.9 \times 10^{-10} (\Delta K^4 - \Delta K_{th}^4) \dots \dots \dots (3)$$

This relationship is indicated by the solid line in Fig. 10 to Fig. 13. The  $\Delta K_{th}$  values were taken as  $6\text{MPa}\sqrt{\text{m}}$  and  $2\text{MPa}\sqrt{\text{m}}$ , and the length of weld crack was 3 mm. It was verified that the influence of weld crack length on calculated results was very slight. Predicted value of fatigue crack initiation life express well the experimental results. Therefore, stress cycles required for the initiation of small crack from blunt weld crack can be predicted by regarding weld crack as real cracks and using the  $da/dN-\Delta K$  relationship and  $\Delta K_{th}$ -value obtained in normal fatigue crack propagation tests.

## 6. CONCLUSIONS

The main findings of this study are summarried as follows.

- (1) Fatigue crack initiates from the deepest point of the weld crack in the direction perpendicular to the stress direction. The angle of the crack initiation can be predicted by using maximum principal stress or minimum strain energy density criterion. The crack initiation angle, therefore, is not influenced by the weld crack angle and the orientation of columnar structure in weld metal. This fact is also verified from the observation of the failure surface.
- (2) Fatigue crack propagates perpendicularly to the stress direction. The path of crack propagation is not influenced by the orientation of the columnar structure in the weld metal.
- (3) Threshold value of fatigue crack initiation from weld crack is same or higher than that of the crack propagation.
- (4) The relationship between fatigue crack growth rate and stress intensity factor range in the weld metal does not depend on the orientation of the columnar structure, and the relationship is similar to that in the case of base steel.

**ACKNOWLEDGEMENT :** The authors sincerely thank Dr. Miki, Tokyo Institute of Technology, for invaluable advices, and Mr. Suzuki and Mr. Endoh, Sakurada-Kikai-Kogyo, for preparation of specimens.

### REFERENCES

- 1) ASME : Boiler and Pressure Vessel Code, Sec. XI, Rule for Inservice Inspection of Nuclear Power Plant Components, 1983.
- 2) BSI : Guidance on Some Methods for the Derivation of Acceptance Levels for Defects in Fusion Welded Joints, PD 6493, 1983.
- 3) JWES : Method of Assessment for Defects in Fusion-Welded Joints with respect to Brittle Fracture, WES 2805, 1980.
- 4) Erdogan, F. and Sih, G. C. : On the Crack Extension in Plates under Plane Loading and Transverse Shear, *Journal of Basic Engineering*, Trans. ASME, Vol. 85, pp. 519-527, 1966.
- 5) Sih, G. C. : Strain-Energy-Density Factor Applied to Mixed Mode Crack Problems, *International Journal of Fracture*, Vol. 10, No. 3, pp. 305-321, 1974.
- 6) Nishitani, H. : Stress Intensity Factor for the Tension of a Semi-Infinite Plate Having an Oblique or a Bent Edge Crack, *Transactions of the JSME*, Vol. 41, No. 344, pp. 1103-1111, 1975 (in Japanese).
- 7) Okumura, T., Nishimura, T., Miki, C. and Hasegawa, K. : Fatigue Crack Growth in Structural Steel, *Proceedings of JSCE*, No. 322, pp. 175-178, 1982.
- 8) Miki, C., Mori, T. and Tajima, J. : Effect of Stress Ratio and Tensile Residual Stress on near Threshold Fatigue Crack Growth, *Proceedings of JSCE*, No. 386, pp. 383-392, 1986.

(Received January 30 1989)